ADVANCED ENERGY MATERIALS

Supporting Information

for *Adv. Energy Mater.,* DOI: 10.1002/aenm.201901469

A Novel Dendrite-Free Mn^{2+}/Zn^{2+} Hybrid Battery with 2.3 V Voltage Window and 11000-Cycle Lifespan

Ming Li, Qiu He, Zilan Li, Qi Li, Yuxin Zhang, Jiashen Meng, Xiong Liu, Shidong Li, Buke Wu, Lineng Chen, Ziang Liu, Wen Luo, Chunhua Han,* and Liqiang Mai**

Supporting Information

A Novel Dendrite-free Mn^{2+}/Zn^{2+} Hybrid Battery with 2.3 V Voltage Window and 11000-Cycle Lifespan

Ming Li, Qiu He, Zilan Li, Qi Li, Yuxin Zhang, Jiashen Meng, Xiong Liu, Shidong Li, Buke Wu, Lineng Chen, Ziang Liu, Wen Luo, Chunhua Han*, Liqiang Mai**

Mr. M. Li, Ms. Q. He, Ms. Z. L. Li, Prof. Q. Li, Ms. Y. X. Zhang, Mr. J. S. Meng, Mr. X. Liu. Mr. S. D. Li, Mr. B. K. Wu, Mr. Z. A. Liu, Ms. W. Luo, Prof. C. H. Han, Prof. L. Q. Mai

State Key Laboratory of Advanced Technology for Materials Synthesis and Processing, Wuhan University of Technology, Hubei, Wuhan 430070, P. R. China

E-mail: mlq518@whut.edu.cn, qi.li@whut.edu.cn; hch5927@gmail.com

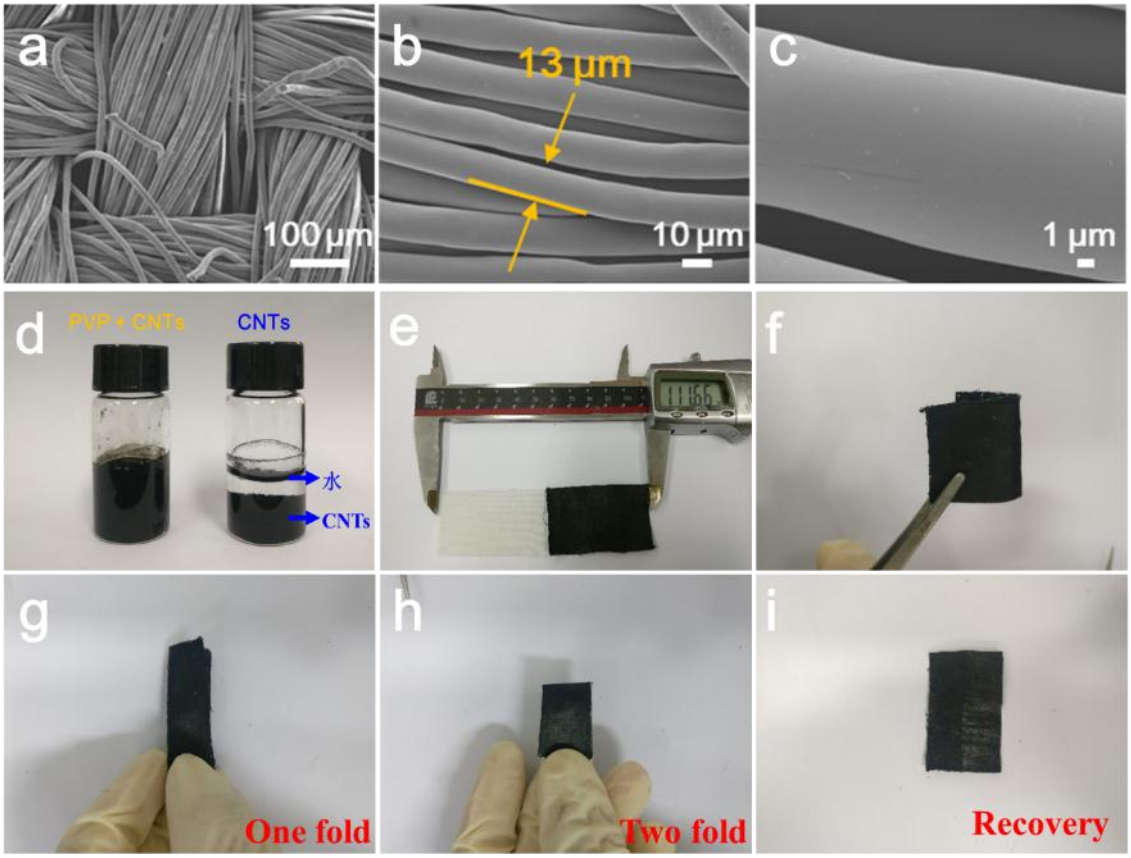

Figure S1. a-c) SEM images of bare polyester cloth. d) Comparison of the configured CNTs ink with/without PVP as additive after an hour of standing. e) The optical images of polyester cloth (white) and polyester-CNTs@MnO_2 (black). f-i) The optical images of flexible polyester-CNTs conductive substrate after different bending states.

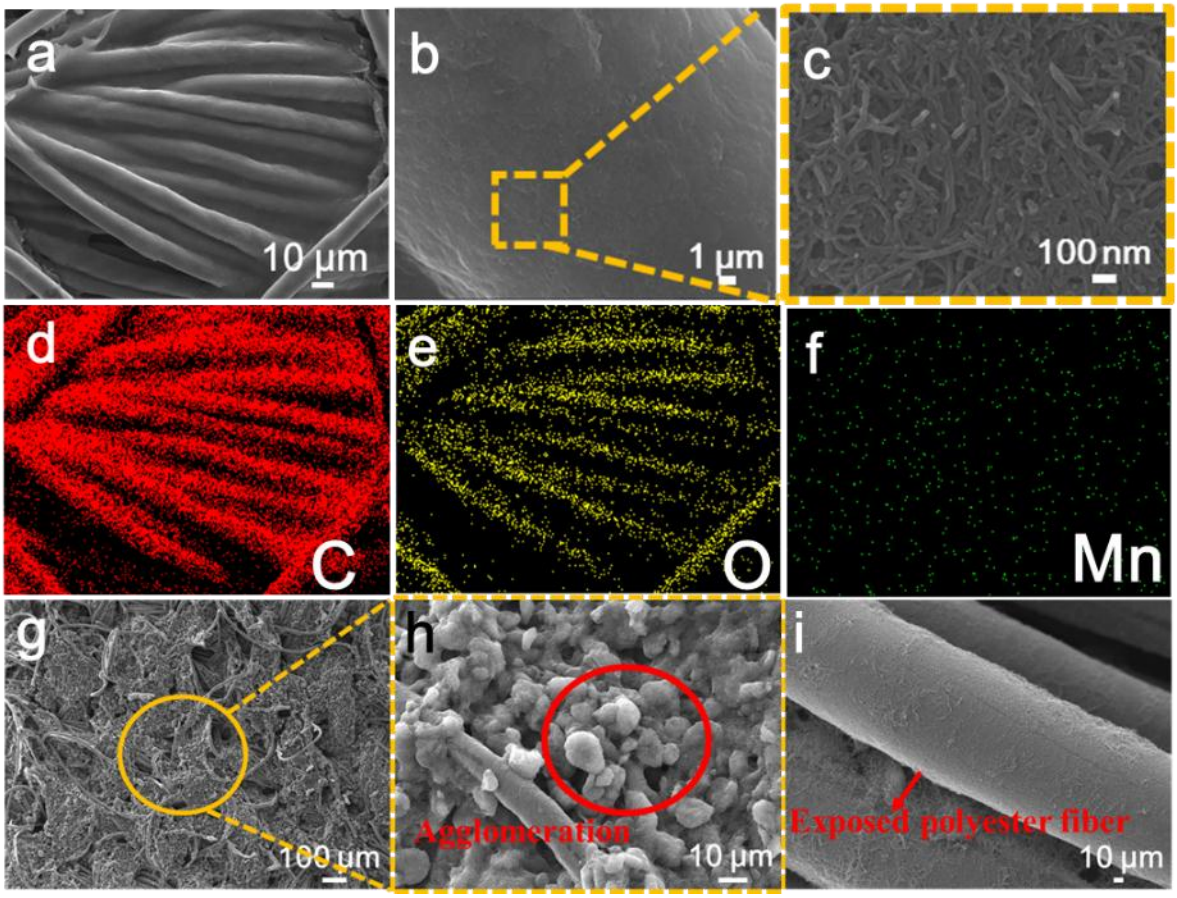

Figure S2. a-c) SEM images of polyester-CNTs. d-f) The corresponding EDS mapping images of C, O, Mn. g-i) SEM images of polyester-CNTs by dipping CNTs ink without PVP as surfactant.

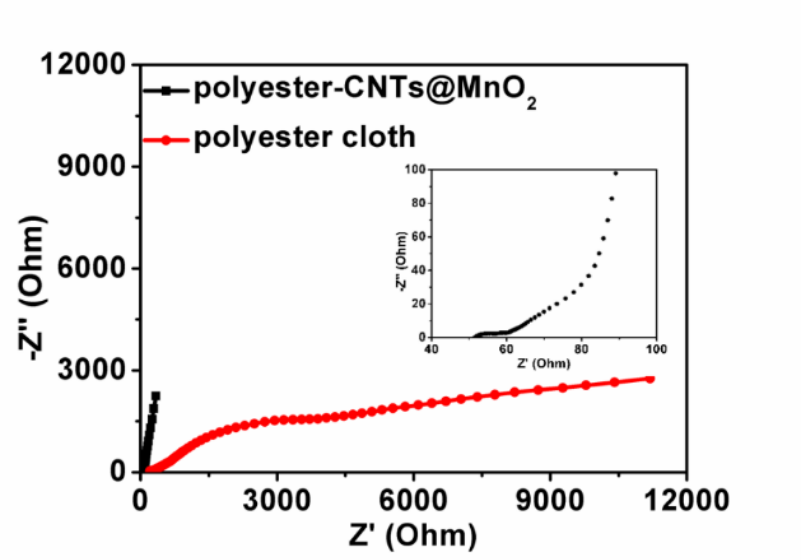

Figure S3. EIS results of conductive polyester-CNTs@MnO_2 and insulating polyester cloth, the insert image is high-resolution EIS of polyester-CNTs@MnO_2.

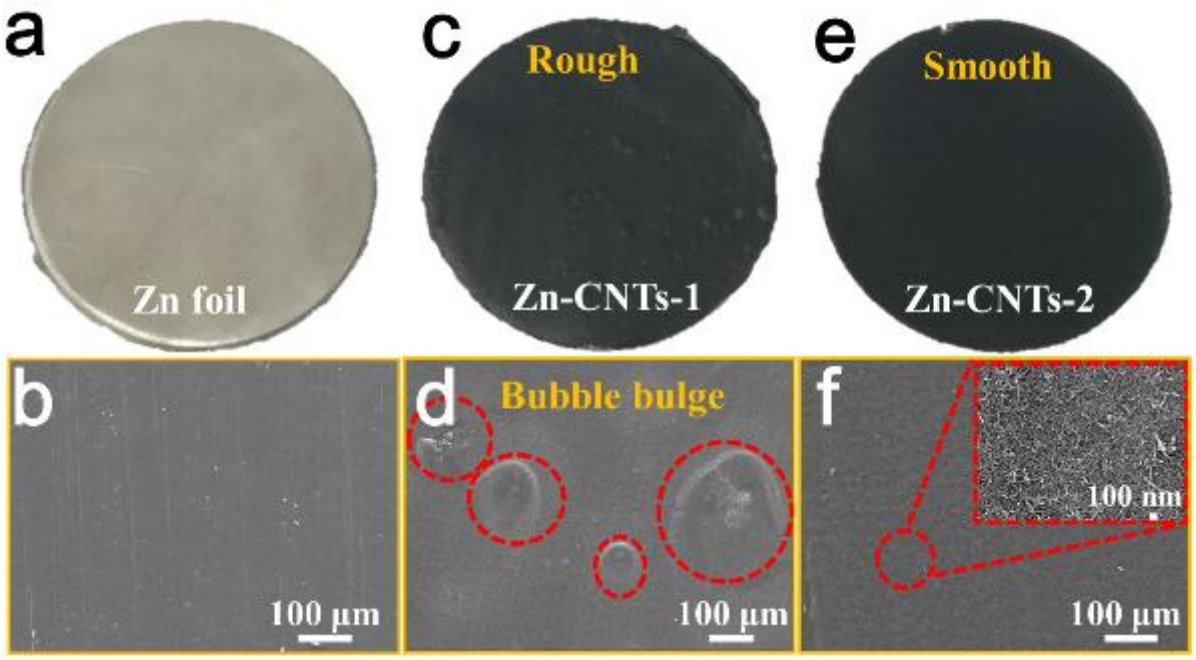

Figure S4. The optical and corresponding SEM images of a,b) Zn foil, c-d) Zn-CNTs-1 prepared by CNTs ink with pure DI water as solvent. e-f) Zn-CNTs-2 prepared by CNTs ink with a ratio of 1:1 alcohol and DI water.

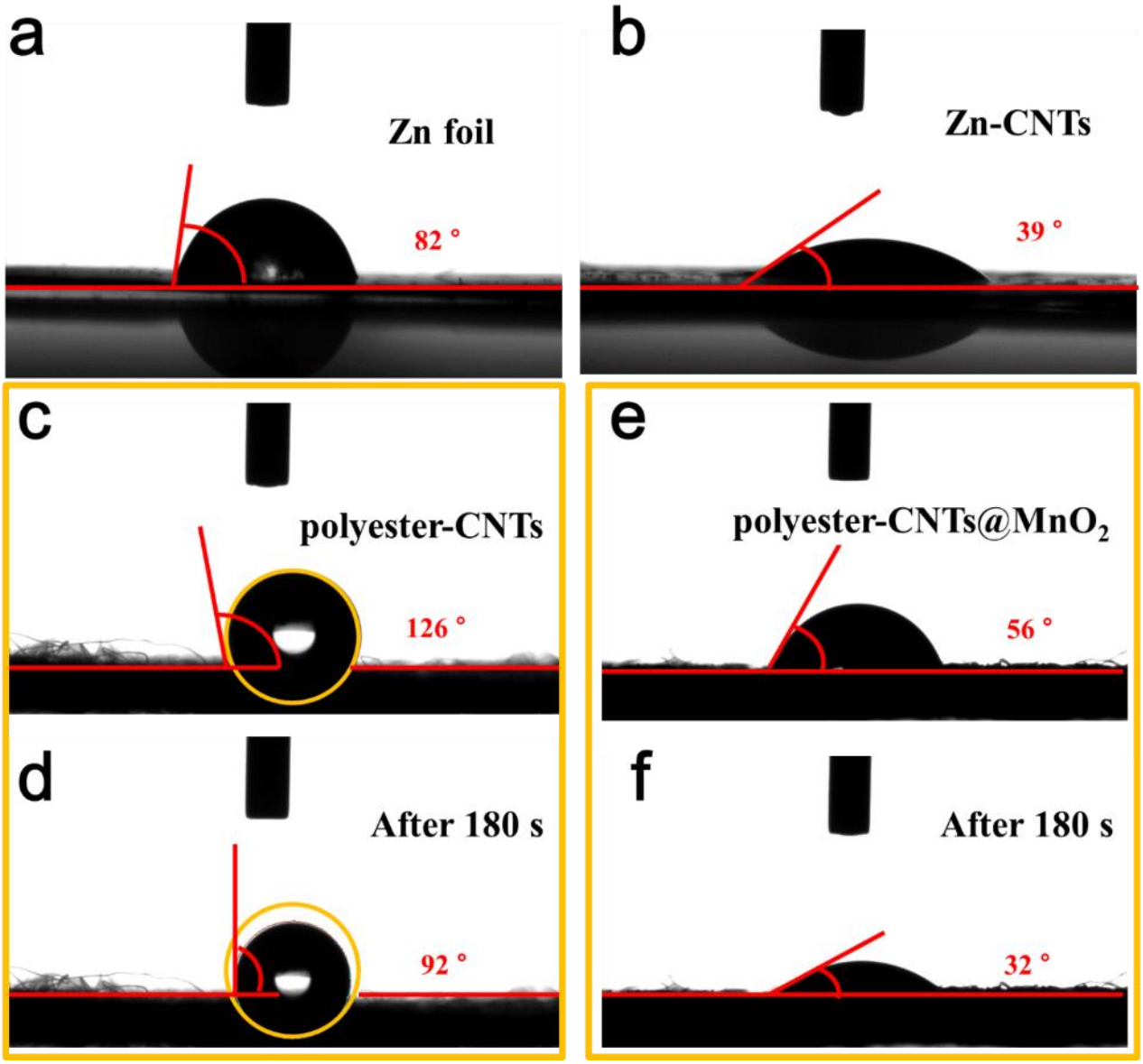

Figure S5. Contact angles of a water droplet on the a) bare Zn foil, b) Zn-CNTs. The change of contact angles on the c-d) polyester-CNTs and e-f) polyester-CNTs@MnO_2 after 3 mins.

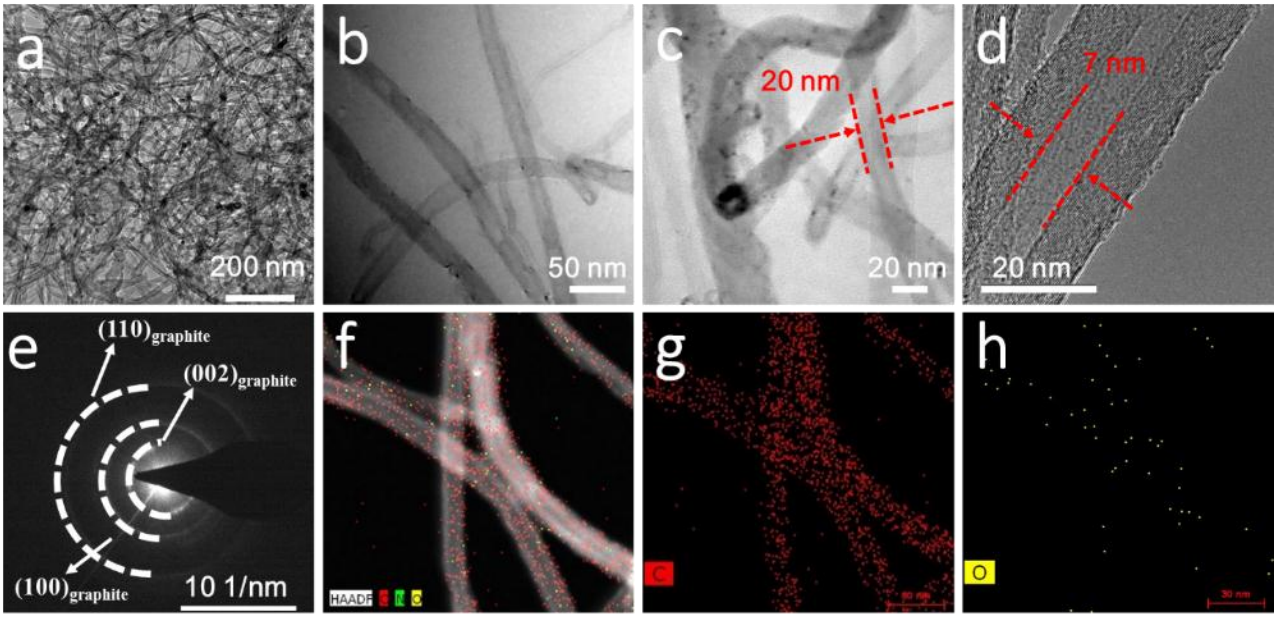

Figure S6. a-d) TEM images of CNTs. e-h) SAED and corresponding EDS mapping images of CNTs.

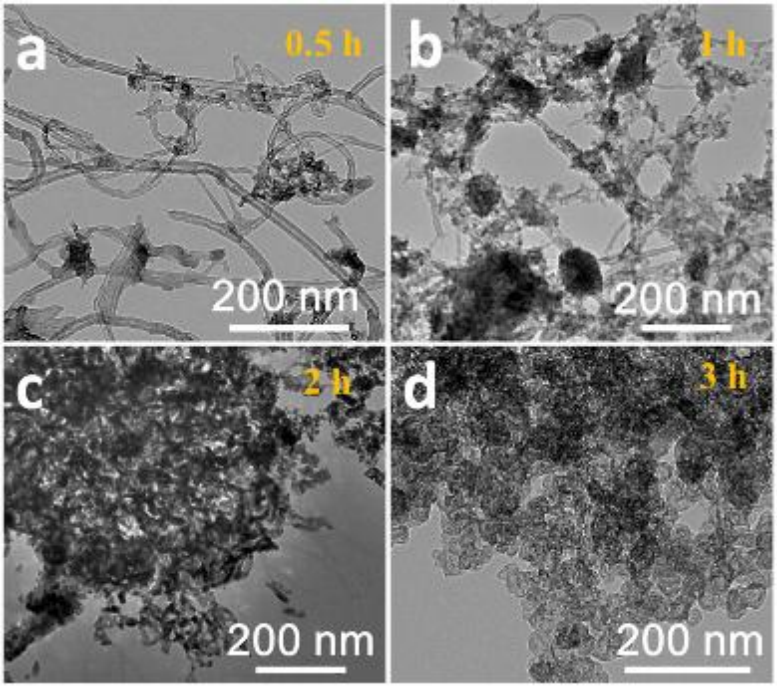

Figure S7. TEM images of polyester-CNTs@MnO_2 at different reaction time a) 0.5 h, b) 1h c) 2h and d) 3h.

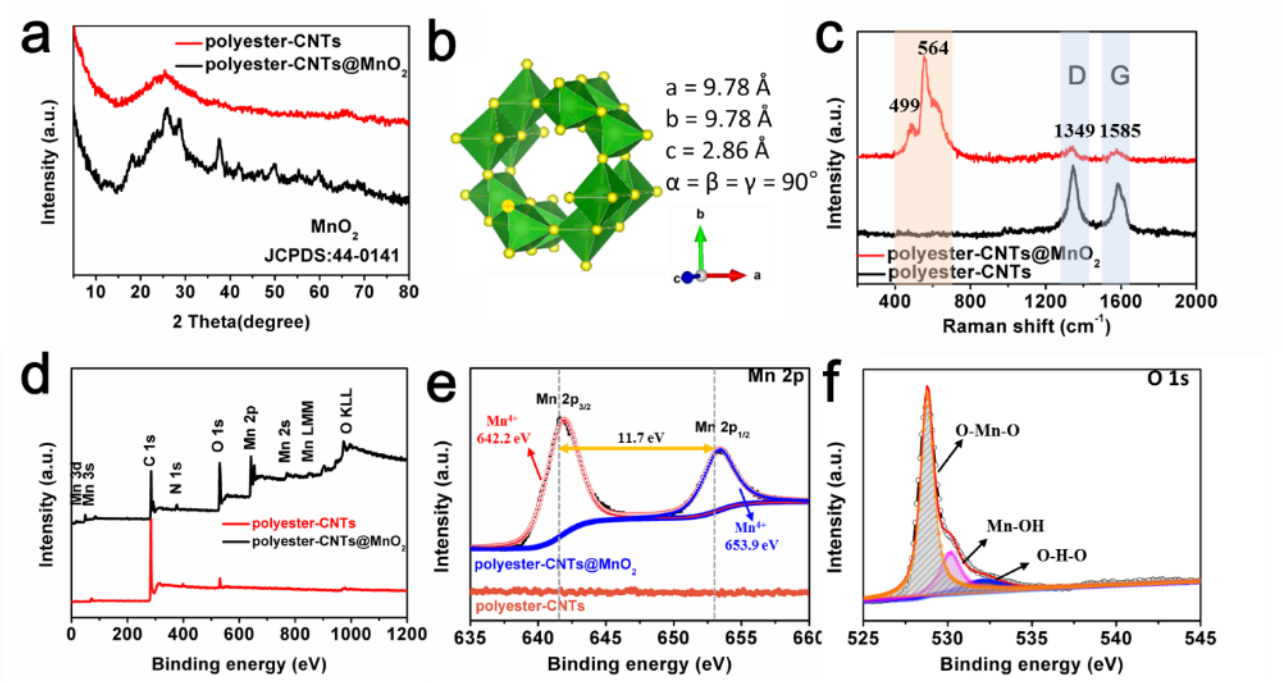

Figure S8. a) XRD results of polyester-CNTs@MnO_2 and polyester-CNTs. b) Top views and crystal structures of MnO_2. (c) Raman spectra, d) XPS full spectra, and e) Mn 2p spectra of polyester-CNTs@MnO_2 and polyester-CNTs. f) O1s spectrum of polyester-CNTs@MnO_2.

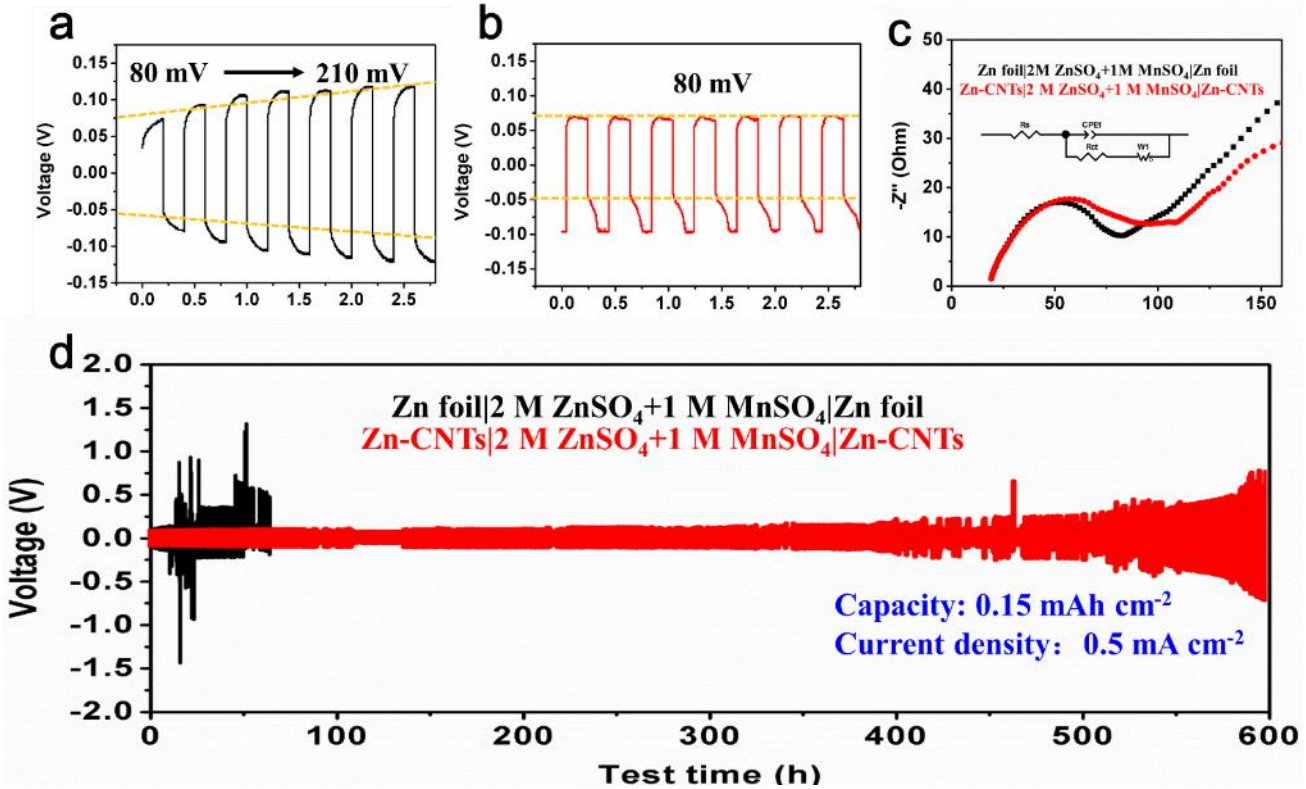

Figure S9. The amount of Zn deposited in each cycle is 0.15 mAh cm^{-2}. The initial cycles of symmetrical cells a) used bare Zn foil or (b) Zn-CNTs as electrode. c) The EIS spectra of Zn symmetric cells used bare Zn and Zn-CNTs as electrode. d) Typical GCD curves of symmetric cells with bare (black) and CNTs-Zn (red) at a current density of 0.5 mA cm^{-2}.

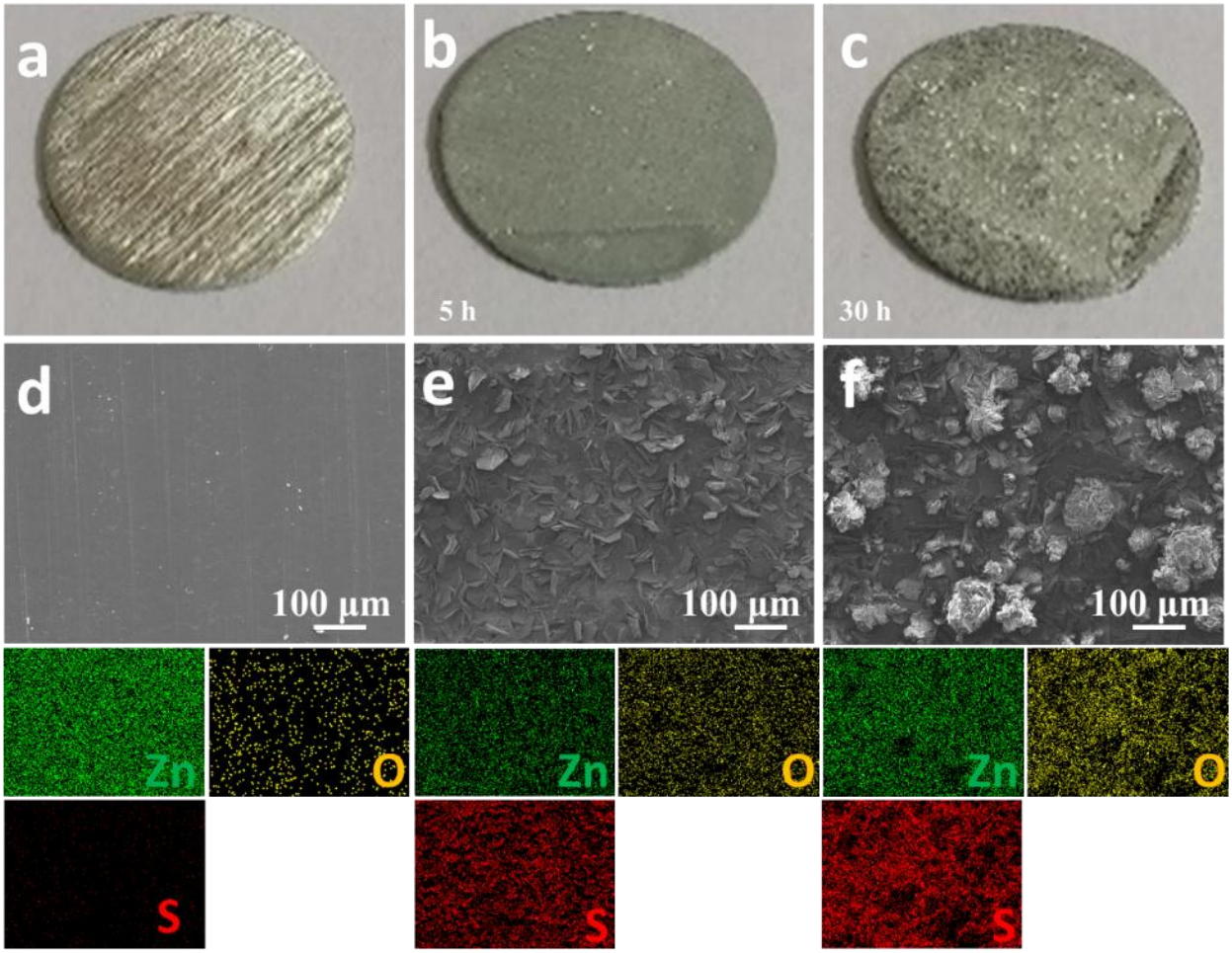

Figure S10. a-c) Optical image changes in the surface morphology of Zn foil during cycling test. d-f) The corresponding SEM images of Zn foil and EDS-mapping images of Zn, O, S.

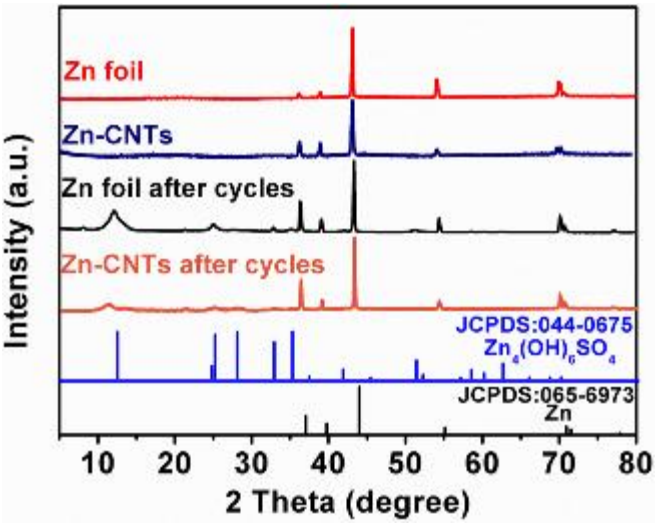

Figure S11. XRD results of bare Zn foil and Zn-CNTs after cycles.

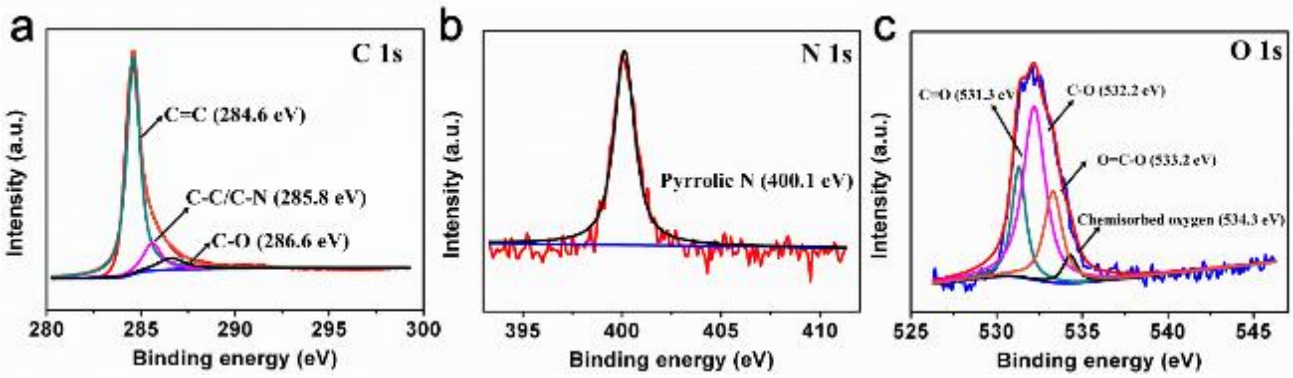

Figure S12. The core-level a) C 1s, b) N 1s and c) O 1s spectra of CNTs.

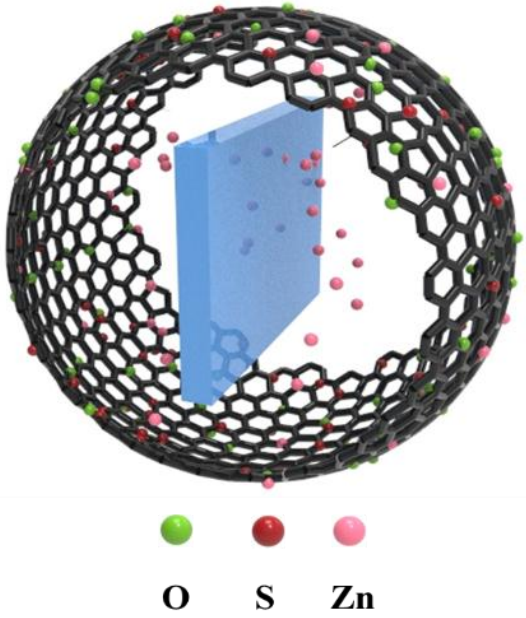

Figure S13. Schematic diagram of the O/S adsorption effect of CNTs protective layer on Zn foil. The green, red, and pink spheres represent O, S, and Zn atoms, respectively. The black networks represent intertwined CNTs protective layer on the surface of Zn. During the charge/discharge processes, the side production of $Zn_4SO_4(OH)_6{\cdot}4H_2O$ appears on the surface of black networks instead of Zn foil. Zn^{2+} ions can pass through CNTs smoothly and deposit uniformly on Zn foil without dendrites.

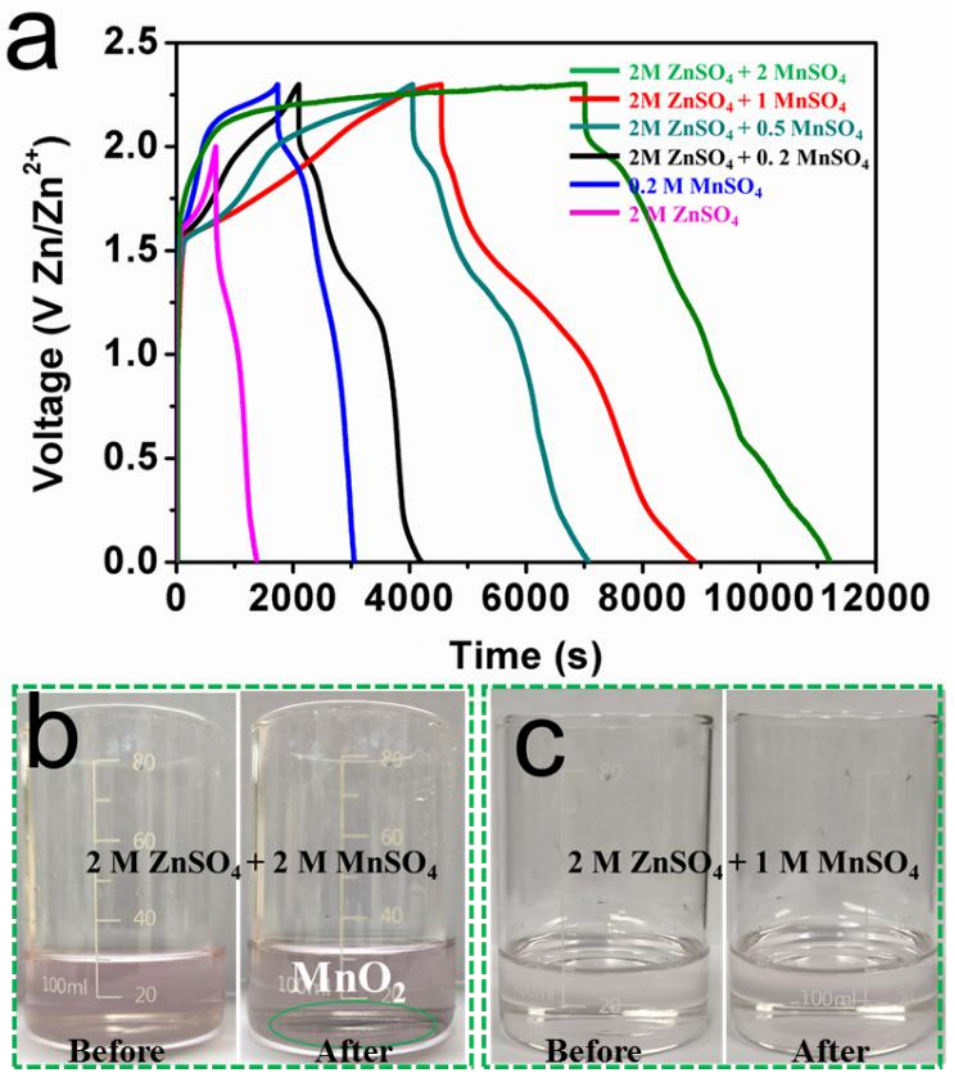

Figure S14. a) GCD curves of Mn^{2+}/Zn^{2+} HB with different electrolytes. The optical images of b) 2 M + 2 M $MnSO_4$, c) 2 M + 1 M $MnSO_4$ after several deposition/dissolution of MnO_2.

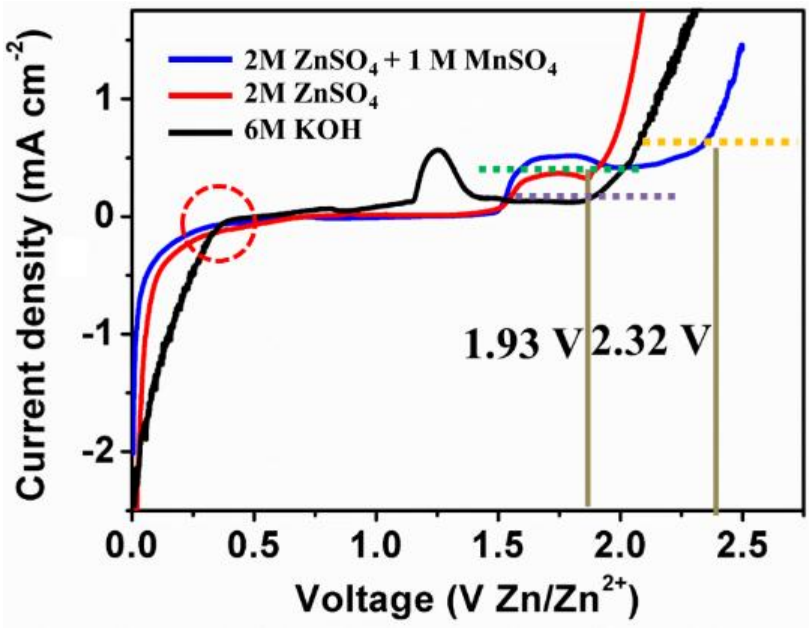

Figure S15. LSV curves of Mn^{2+}/Zn^{2+} HB in different electrolytes to evaluate the voltage of oxygen production.

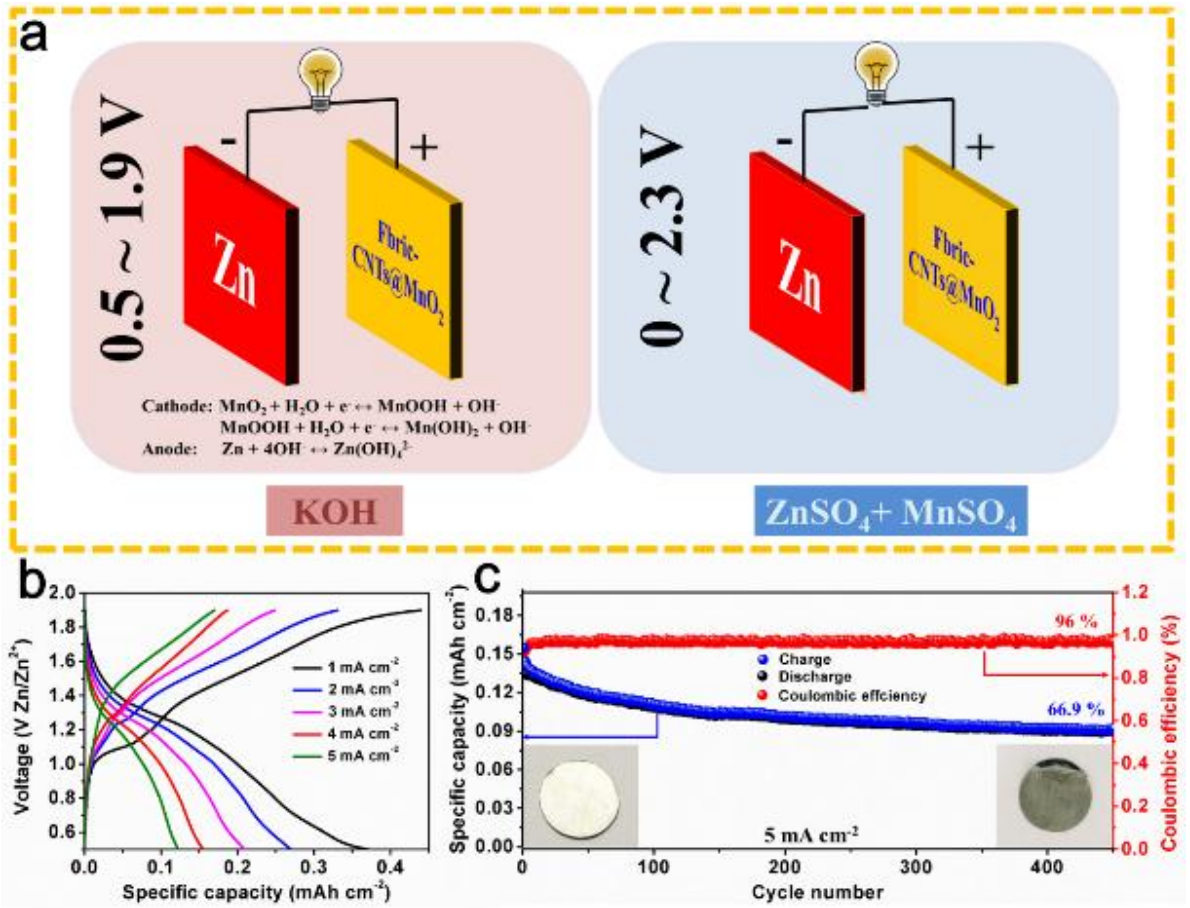

Figure S16. a) Schematic illustration of Mn^{2+}/Zn^{2+} HB in alkaline and mild electrolytes. b) GCD curves and c) cycling performance of Zn-MnO_2 alkaline battery in 6 M KOH.

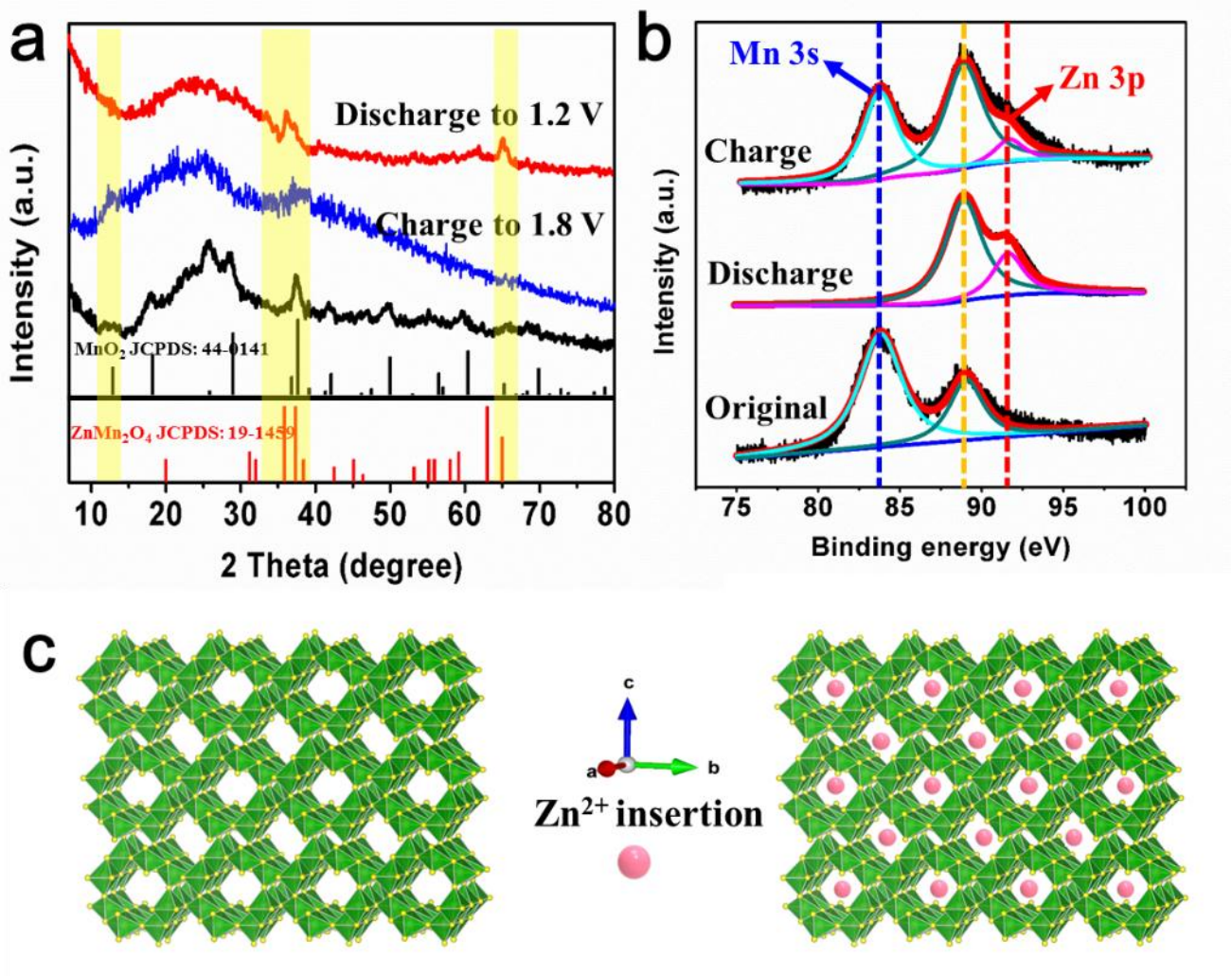

Figure S17. a) XRD results, b) Mn 3s spectra of polyester-CNTs@MnO_2 at Zn^{2+} ion insertion (discharge to 1.2 V) and extraction conditions (charge to 1.8 V). c) Schematic illustration of the Zn^{2+} ion intercalation mechanism of polyester-CNTs@MnO_2 cathode.

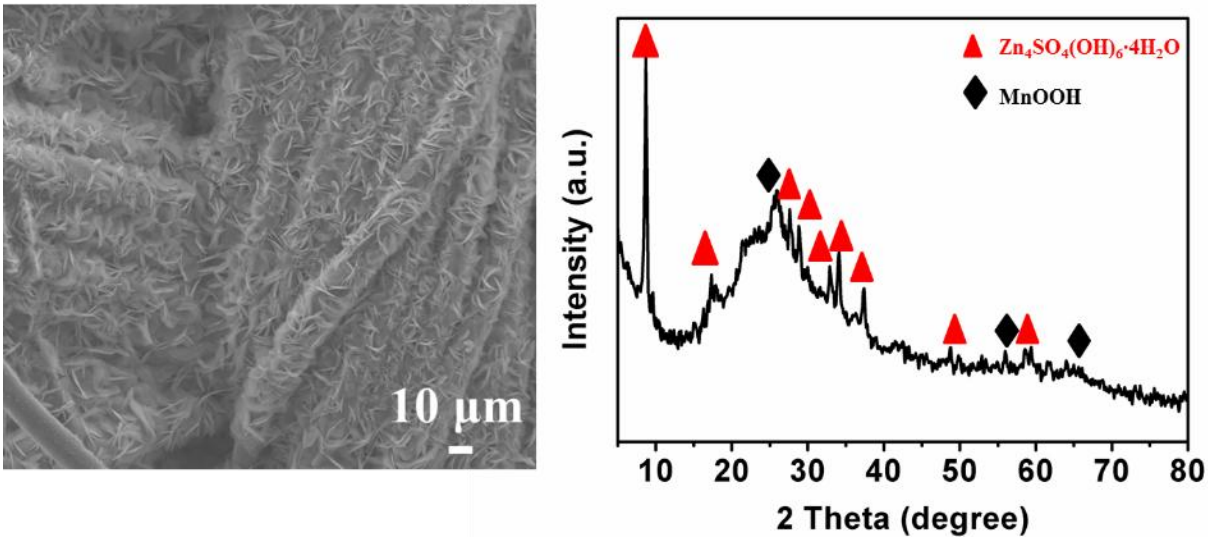

Figure S18. SEM images of flake-like $Zn_4SO_4(OH)_6{\cdot}4H_2O$ on polyester-CNTs@MnO_2 and XRD result at 0 V.

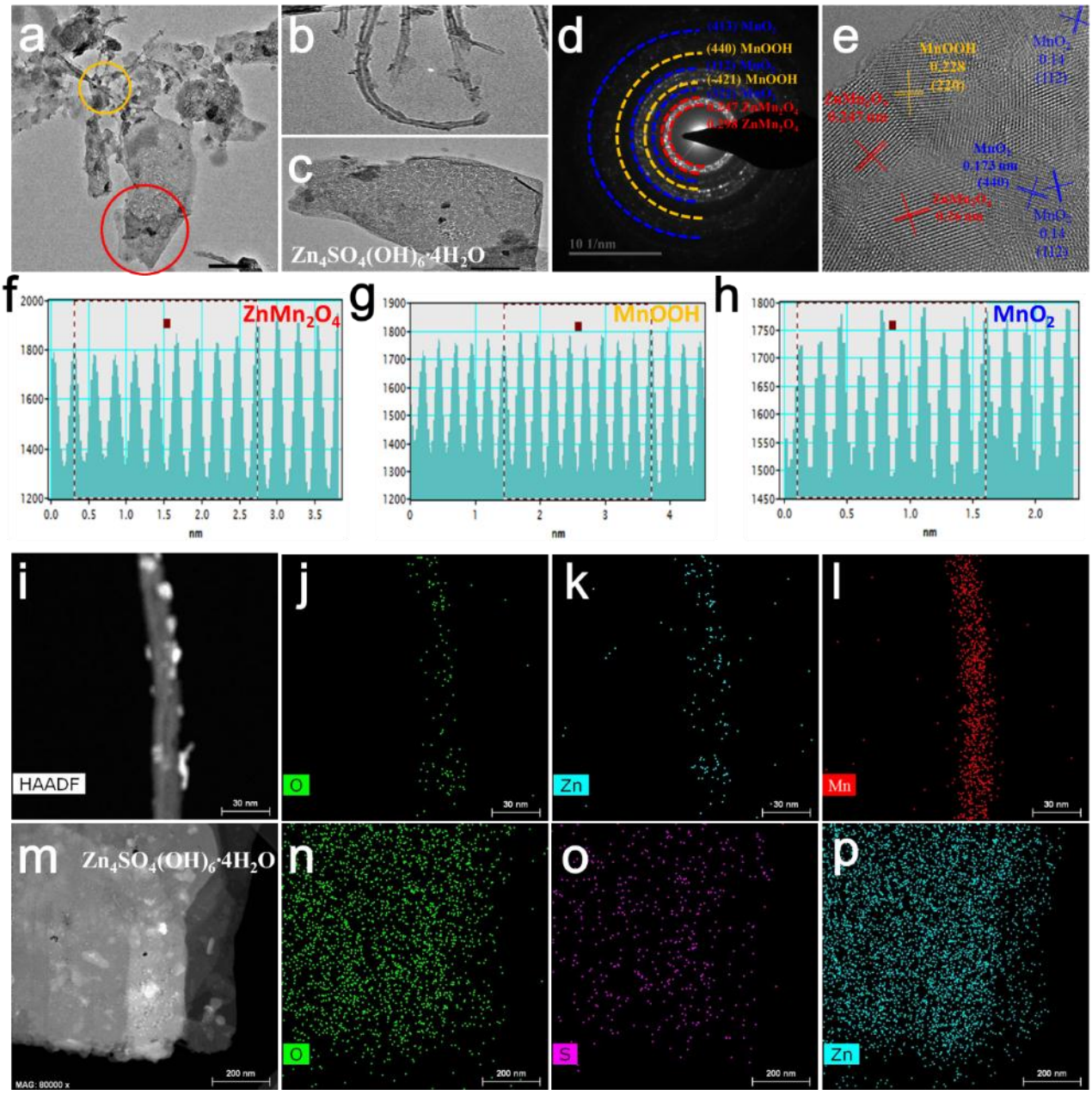

Figure S19. a-c) TME images after discharge to 0 V, d-e) corresponding SEAD and high-resolution images of polyester-CNTs@MnO_2. f-h) Lattice spacing diagram of different components of $ZnMn_2O_4$, MnOOH, and MnO_2. The EDS mapping images of i-l) O, Zn, Mn in CNTs@MnO_2 and m-p) O,S, Zn in $Zn_4SO_4(OH)_6{\cdot}4H_2O$.

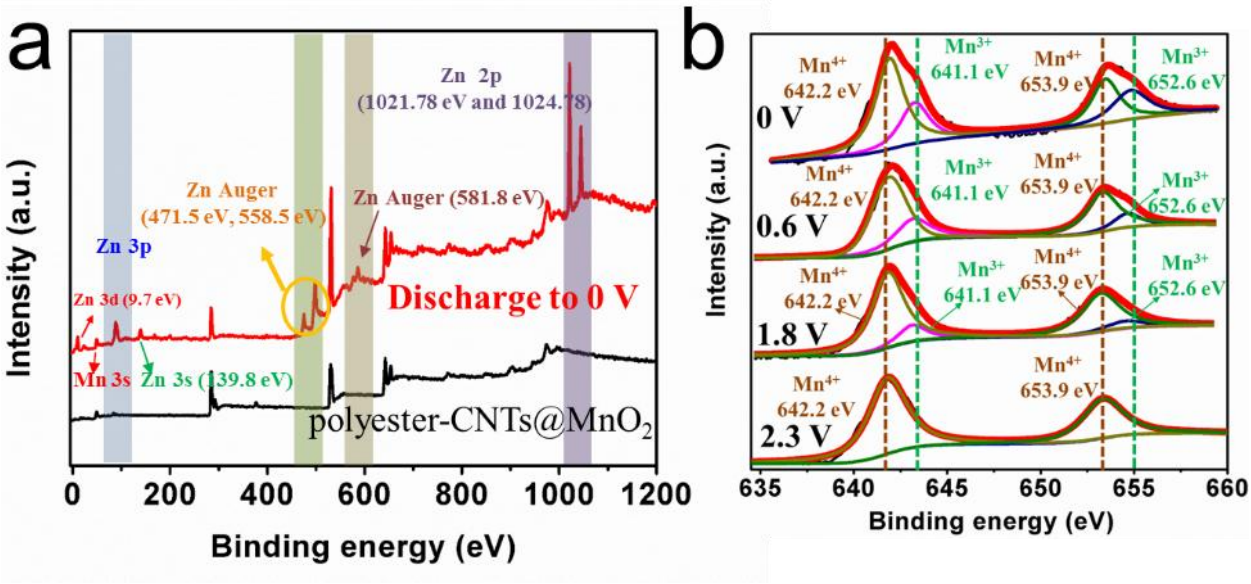

Figure S20. a) XPS full spectra of polyester-CNTs@MnO_2 (original and discharge to 0V). b) The core-level Mn 2p spectra of polyester-CNTs@MnO_2 from 2.3 to 0 V during the discharge process.

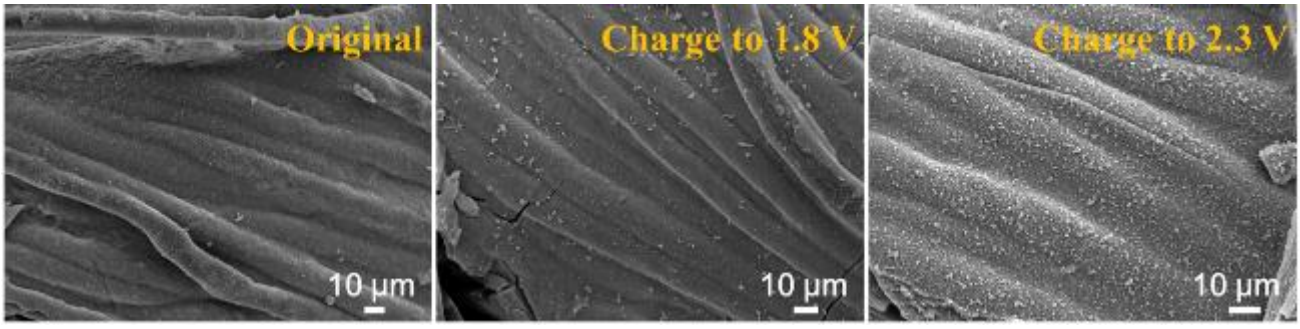

Figure S21. SEM images of polyester-CNTs@MnO_2 cathode during the charging process.

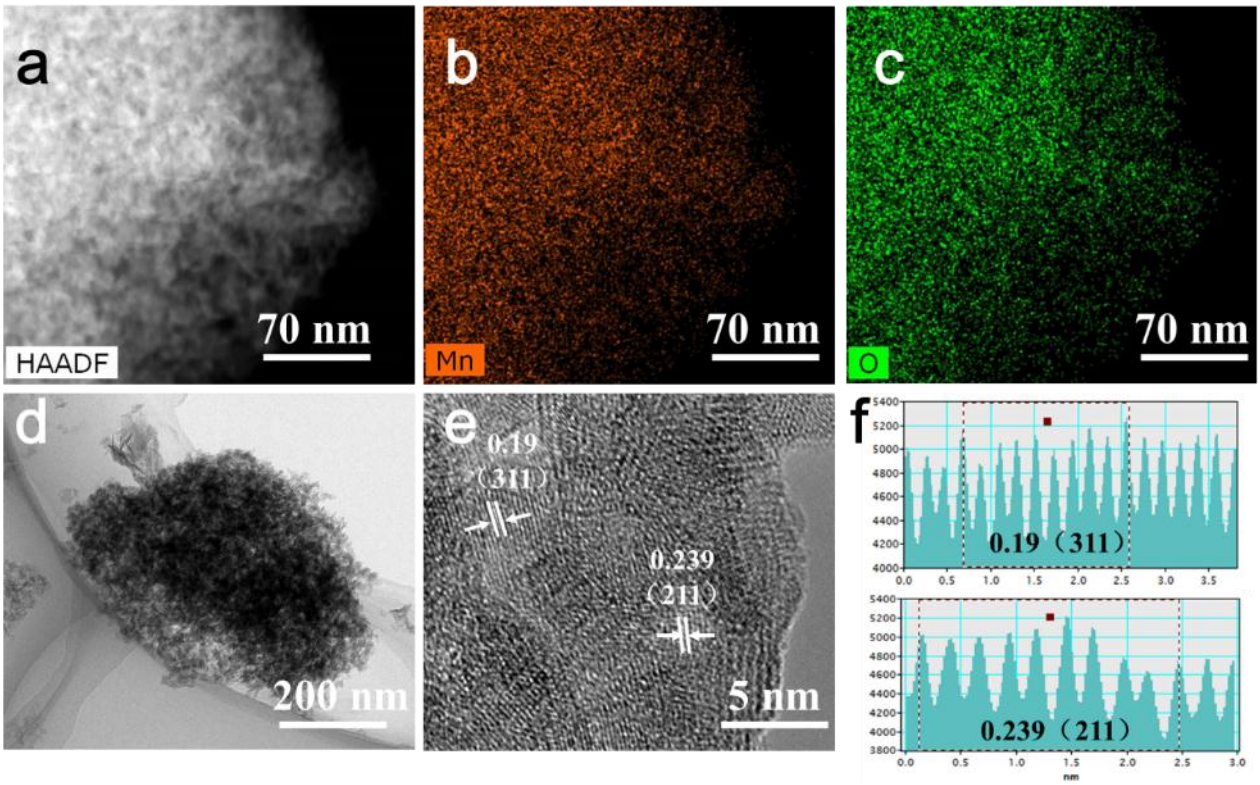

Figure S22. a-c) TEM and corresponding EDS mapping images. d-f) The high-resolution images and Lattice spacing diagram of deposited MnO_2.

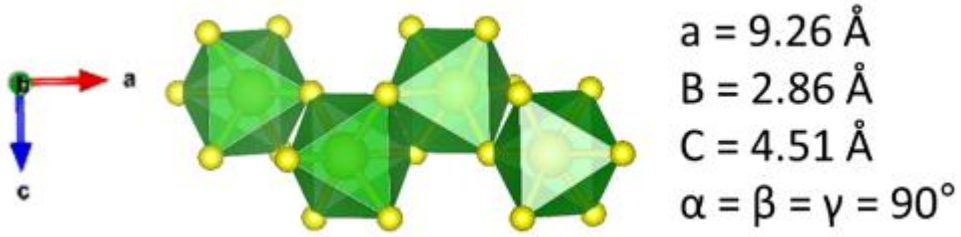

Figure S23. The crystal structures of deposited MnO_2 with side views.

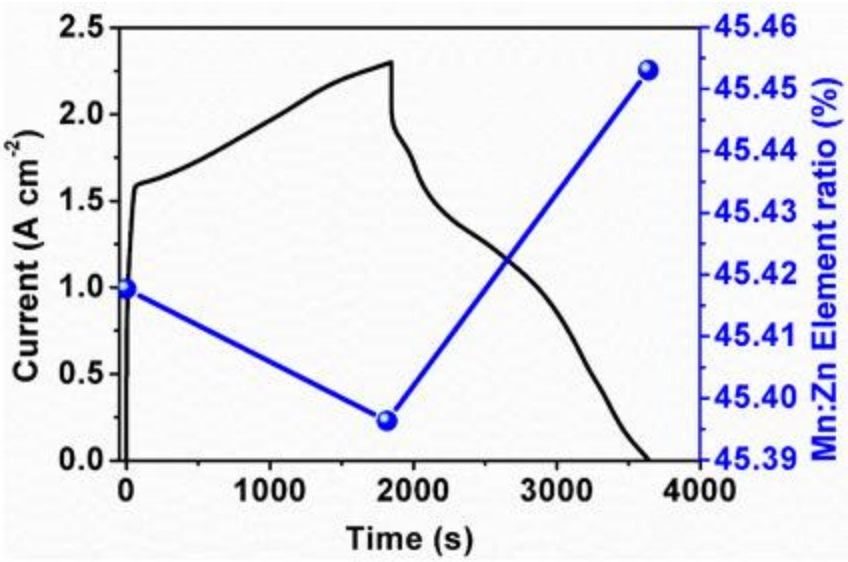

Figure S24. Element analysis the ratio of Zn^{2+} and Mn^{2+} in a 2 M $ZnSO_4$ + 1 M $MnSO_4$ aqueous electrolyte.

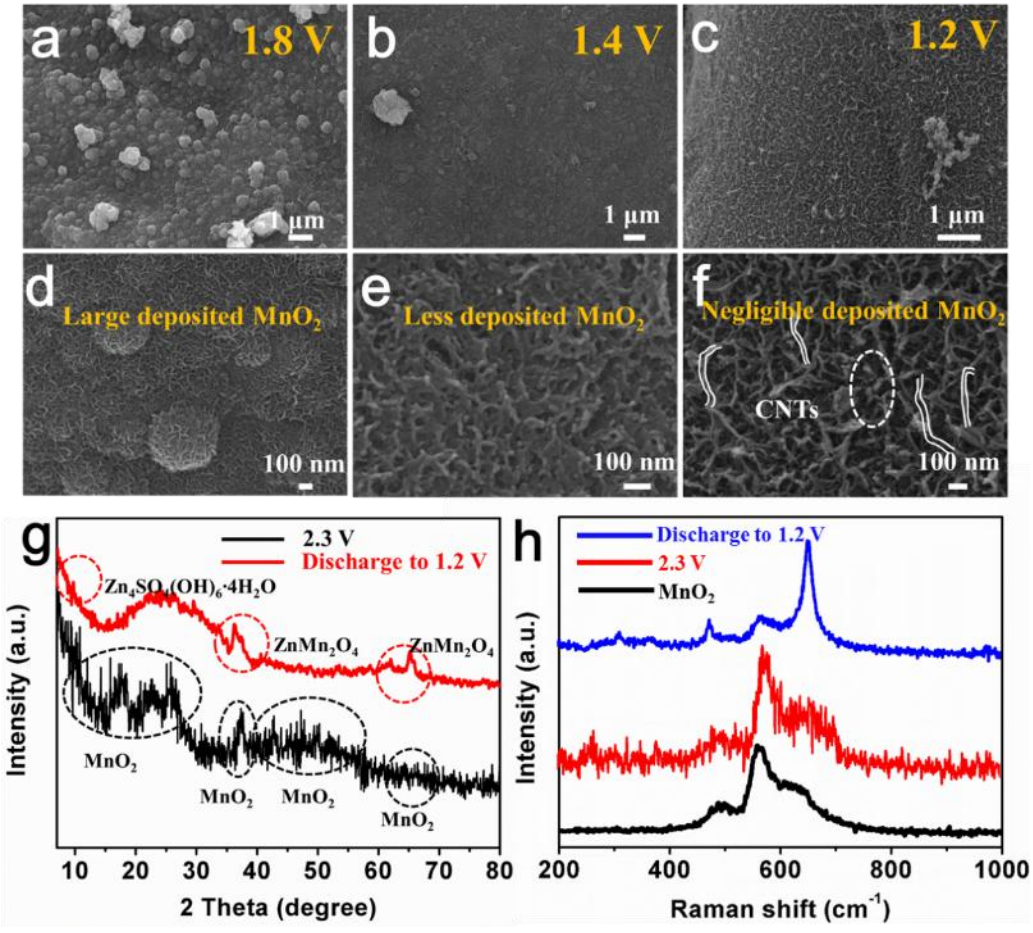

Figure S25. The SEM images of cathode at different discharge state of a,d)1.8 V, b,e)1.4 V, and c,f)1.2 V respectively. g) XRD patterns of 2.3 V and discharge to 1.2 V. h) Raman spectra of MnO_2, cathode at 2.3V and discharge to 1.2V. During the discharge process of the deposited MnO_2 gradually disappears and obvious CNTs can be clearly seen at 1.2 V. It indicates that the deposited MnO_2 has been substantially converted into Mn^{2+} ion and returned to the electrolyte solution. Correspondingly, the XRD pattern at 1.2 V show the peaks of deposited MnO_2 is obviously weakened, which is supported by Raman spectra.

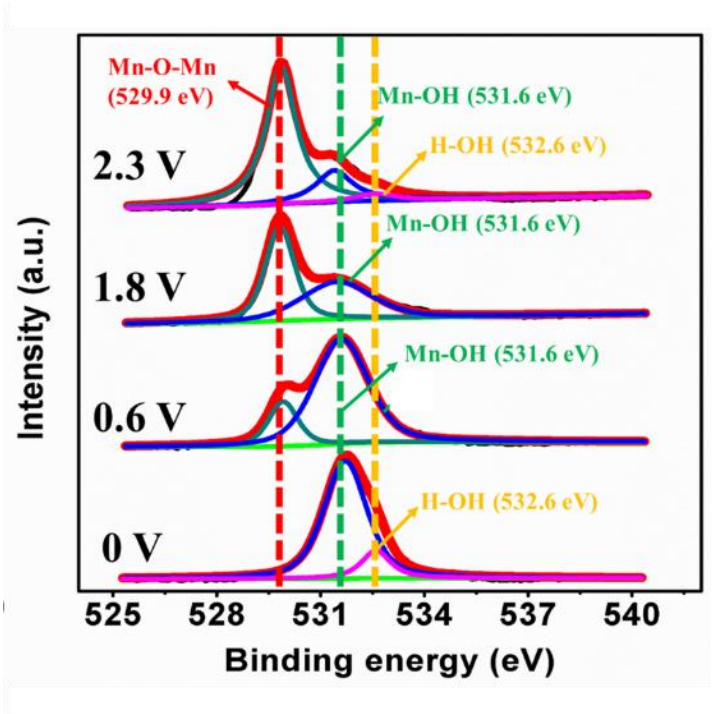

Figure S26. O 1s core-level XPS spectra of the polyester-CNT@MnO_2 electrode at different states (discharge process from 2.3 to 0 V).

Table S1. Comparison of our Mn^{2+}/Zn^{2+} HB with other recently reported aqueous batteries.

Aqueous batteries	Electrolyte	Capacity retention	Specific areal capacity	Voltage window	Ref.
Ni-Zn	1 M KOH +0.02	92.5% after 1800	0.422 mAh cm^{-2}	1.4~2.0 V	[1]

battery	$Zn(Ac)_2$	cycles at 8 mA cm^{-2}	at 8 mA cm^{-2}		
Ni-Zn battery	2 M KOH saturated with ZnO	72.9% after 2400 cycle at 8 mA cm^{-2}	0.422 mAh cm^{-2} at 0.5 mA cm^{-2}	1.4~1.95 V	[2]
Zn-MnO_2 battery	2 M $ZnCl_2$+0.4 M $MnSO_4$	83.7% after 300 cycles at 6 mA cm^{-2}	1.97 mAh cm^{-2} at 4 mA cm^{-2}	1~1.8 V	[3]
Zn-Co_3O_4 battery	2 M $ZnSO_4$ + 0.2 M $CoSO_4$	92% after 5000 cycles at 4 mA cm^{-2}	0.158 mAh cm^{-2} at 1 mA cm^{-2}	0.8~2.2 V	[4]
Zn-MnO_2 battery	2 M $ZnCl_2$+0.4 M $MnSO_4$	93.6% after 1000 cycles at 3.2 mA cm^{-2}	1.12 mAh cm^{-2} at 1.6 mA cm^{-2}	1~1.8 V	[5]
Zn-PTO battery	2 M $ZnSO_4$	100% after 1000 cycles 15 mA cm^{-2}	1.68 mAh cm^{-2} at 0.2 mA cm^{-2}	0.4~1.5 V	[6]
Zn-PANS battery	1 M $ZnSO_4$	84.6% after 2000 cycles at 60 mA cm^{-2}	0.22 mAh cm^{-2} at 0.24 mA cm^{-2}	0.5~1.6 V	[7]
Ni-Fe battery	6 M KOH	78% after 2000 cycles at 7.8 mA cm^{-2}	0.708 mAh cm^{-2} at 1.8 mA cm^{-2}	0~1.6 V	[8]
Zn-$NiCo_2O_4$ battery	1 M KOH +0.05 $Zn(Ac)_2$	74% after 5000 cycles at 16.7 mA cm^{-2}	0.24 mAh cm^{-2} at 2 mA cm^{-2}	1.4~1.9 V	[9]
Zn-PANI battery	1 M $Zn(CF_3SO_3)_2$	92% after 3000 cycles at 7.5 mA cm^{-2}	0.286 mAh cm^{-2} at 0.075 mA cm^{-2}	0.5~1.6 V	[10]

Zn-ZOV battery	2M $ZnSO_4$	89% after 2000 cycles at 22.4 mA cm^{-2}	1.14 mAh cm^{-2} at 0.56 mA cm^{-2}	0.4~1.4 V	[11]
NH_4-Ion battery	1 M $(NH_4)_2SO_4$	74% after 2000 cycles at 1.05 mA cm^{-2}	0.21 mAh cm^{-2} at 0.525 mA cm^{-2}	0.2~0.9 V	[12]
Zn-Co battery	6 M KOH +1.5 M ZnO	71.1% after 5000 cycles at 80 mA cm^{-2}	0.71 mAh cm^{-2} at 1 mA cm^{-2}	1.2~1.95 V	[13]
Ni-Bi battery	1 M KOH	89% after 1000 cycles at 5.7 mA cm^{-2}	0.081 mAh cm^{-2} at 1 mA cm^{-2}	0~1.6 V	[14]
Mn–H battery	1 M $MnSO_4$ + 0.05 M H_2SO_4	100% after 10000 cycles at 10 mA cm^{-2}	1 mAh cm^{-2} at 10 mA cm^{-2}	0.5~1.6 V	[15]
Aqueous Li^+ battery	2 M $LiNO_3$	72% after 1000 cycles at 22 mA cm^{-2}	0.88 mAh cm^{-2} at 4.4 mA cm^{-2}	0~2.0 V	[16]
Aqueous Li^+ battery	5 M $LiNO_3$	94% after 100 cycles at 3 mA cm^{-2}	0.32 mA cm^{-2} at 1 mA cm^{-2}	0.2 ~1.4 V	[17]
Ni-Fe battery	1 M KOH	70.5% after 2000 cycles	0.39 mAh cm^{-2} at 5 mA cm^{-2}	0~1.6 V	[18]
Ni-Zn battery	1 M KOH	90% after 5000 cycles at 12.8 mA cm^{-2}	0.46 mAh cm^{-2} at 1.6 mA cm^{-2}	1.4~2.0 V	[19]
Our work	2 M $ZnSO_4$ + 1 M	100% after 11000	0.96 mAh cm^{-2} at	0~2.3V	

$MnSO_4$	cycles at 5 mA cm^{-2}	1 mA cm^{-2}	

Reference.

[1] R. Wang, Y. Han, Z. Wang, J. Jiang, Y. Tong and X. Lu, *Adv. Funct. Mater.* **2018**, 28, 1802157.

[2] J. Liu, C. Guan, C. Zhou, Z. Fan, Q. Ke, G. Zhang, C. Liu and J. Wang, *Adv. Mater.* **2016**, 28, 8732.

[3] Y. Zeng, X. Zhang, Y. Meng, M. Yu, J. Yi, Y. Wu, X. Lu and Y. Tong, *Adv. Mater.* **2017**, 29, 1700274.

[4] L. Ma, S. Chen, H. Li, Z. Ruan, Z. Tang, Z. Liu, Z. Wang, Y. Huang, Z. Pei, J. A. Zapien and C. Zhi, *Energy Environ. Sci.* **2018**, 11, 2521-2530.

[5] W. Qiu, Y. Li, A. You, Z. Zhang, G. Li, X. Lu and Y. Tong, *J. Mater. Chem. A* **2017**, 5, 14838.

[6] Z. Guo, Y. Ma, X. Dong, J. Huang, Y. Wang and Y. Xia, *Angew. Chem. Int. Ed.* **2018**, 57, 11737.

[7] H. Y. Shi, Y. J. Ye, K. Liu, Y. Song and X. Sun, *Angew. Chem. Int. Ed.* **2018**, 57, 16359.

[8] J. Liu, M. Chen, L. Zhang, J. Jiang, J. Yan, Y. Huang, J. Lin, H. J. Fan and Z. X. Shen, *Nano Lett.* **2014**, 14, 7180.

[9] Y. Zeng, Z. Lai, Y. Han, H. Zhang, S. Xie and X. Lu, *Adv. Mater.* **2018**, 30, 1802396.

[10] F. Wan, L. Zhang, X. Wang, S. Bi, Z. Niu and J. Chen, *Adv. Funct. Mater.* **2018**, 28, 1804975.

[11] D. Chao, C. R. Zhu, M. Song, P. Liang, X. Zhang, N. H. Tiep, H. Zhao, J. Wang, R. Wang, H. Zhang and H. J. Fan, *Adv. Mater.* **2018**, 30, 1803181.

[12] X. Wu, Y. Qi, J. J. Hong, Z. Li, A. S. Hernandez and X. Ji, *Angew. Chem. Int. Ed.* **2017**, 56, 13026.

[13] M. Li, J. Meng, Q. Li, M. Huang, X. Liu, K. A. Owusu, Z. Liu and L. Mai, *Adv. Funct. Mater.* **2018**, 28, 1802016.

[14] Y. Zeng, Z. Lin, Y. Meng, Y. Wang, M. Yu, X. Lu and Y. Tong, *Adv Mater.* **2016**, 28, 9188-9195.

[15] W. Chen, G. Li, A. Pei, Y. Li, L. Liao, H. Wang, J. Wan, Z. Liang, G. Chen, H. Zhang, J. Wang

and Y. Cui, *Nat. Energy* **2018**, 3, 428.

[16] X. Dong, L. Chen, X. Su, Y. Wang and Y. Xia, *Angew. Chem. Int. Ed.* **2016**, 55, 7474.

[17] Z. Liu, H. Li, M. Zhu, Y. Huang, Z. Tang, Z. Pei, Z. Wang, Z. Shi, J. Liu, Y. Huang and C. Zhi, *Nano Energy* **2018**, 44, 164.

[18] C. Guan, W. Zhao, Y. Hu, Q. Ke, X. Li, H. Zhang and J. Wang, *Adv. Energy Mater.* **2016**, 6, 1601034.

[19] C. Xu, J. Liao, C. Yang, R. Wang, D. Wu, P. Zou, Z. Lin, B. Li, F. Kang and C.-P. Wong, *Nano Energy* **2016**, 30, 900.